

Abolished synthesis of cholic acid reduces atherosclerotic development in apolipoprotein E knockout mice^S

Katharina Slätis,^{1,*} Mats Gåfvels,^{1,2,*} Kristina Kannisto,^{*} Olga Ovchinnikova,[†] Gabrielle Paulsson-Berne,[†] Paolo Parini,^{*} Zhao-Yan Jiang,^{*} and Gösta Eggertsen^{*}

Unit for Clinical Chemistry, Department of Laboratory Medicine^{*} and Centre for Molecular Medicine,[†] Karolinska Institutet, Stockholm, Sweden

Abstract To investigate the effects of abolished cholic acid (CA) synthesis in the *ApoE* knockout model [apolipoprotein E (apoE) KO], a double-knockout (DKO) mouse model was created by crossbreeding *Cyp8b1* knockout mice (*Cyp8b1* KO), unable to synthesize the primary bile acid CA, with apoE KO mice. After 5 months of cholesterol feeding, the development of atherosclerotic plaques in the proximal aorta was 50% less in the DKO mice compared with the apoE KO mice. This effect was associated with reduced intestinal cholesterol absorption, decreased levels of apoB-containing lipoproteins in the plasma, enhanced bile acid synthesis, reduced hepatic cholesteryl esters, and decreased hepatic activity of ACAT2. The upregulation of *Cyp7a1* in DKO mice seemed primarily caused by reduced expression of the intestinal peptide FGF15. Treatment of DKO mice with the farnesoid X receptor (FXR) agonist GW4064 did not alter the intestinal cholesterol absorption, suggesting that the action of CA in this process is confined mainly to formation of intraluminal micelles and less to its ability to activate the nuclear receptor FXR. **Inhibition of CA synthesis may offer a therapeutic strategy for the treatment of hyperlipidemic conditions that lead to atherosclerosis.**—Slätis, K., M. Gåfvels, K. Kannisto, O. Ovchinnikova, G. Paulsson-Berne, P. Parini, Z-Y. Jiang, and G. Eggertsen. **Abolished synthesis of cholic acid reduces atherosclerotic development in apolipoprotein E knockout mice.** *J. Lipid Res.* 2010. 51: 3289–3298.

Supplementary key words atherosclerosis • bile acids • metabolism

The pathogenesis of atherosclerosis is a multifactorial process comprising a number of pathological conditions, such as dyslipidemia, lipid deposition in the arterial wall, inflammation, cell migration, and thrombosis formation (1). The role of bile acids in this disease process also de-

serves attention, inasmuch as bile acids tightly regulate cholesterol homeostasis. The hepatobiliary system constitutes a major clearance pathway for excess cholesterol, which is eliminated into the fecal route either through conversion of cholesterol into bile acids or by direct secretion of cholesterol in the bile. Cholic acid (CA), one of the major primary bile acids in both man and rodents, is assigned a number of functions within this metabolic route. Intestinal absorption of cholesterol is promoted by CA, which in its role as a specific ligand for the nuclear farnesoid X receptor (FXR), regulates the expression of a large number of genes within the lipid metabolism and also the carbohydrate metabolism [for a review, see Lefebvre et al. (2)]. The contribution of the small intestine in the regulation of cholesterol metabolism and in the development of atherosclerosis is underlined by the observation that high dietary administration of cholesterol, with or without cholate supplementation, accelerates the vascular lesions in apolipoprotein E (*ApoE*) knockout mice (apoE KO) (3), a commonly used animal model for atherosclerosis [for a review, see Meir and Leitersdorf (4)].

The direct uptake of cholesterol in the small intestine is mainly mediated by NPC1L1 [for a review see Davis and Altmann (5)]. Nevertheless, CA also plays a role in intestinal cholesterol absorption, because it promotes the uptake by inclusion of luminal cholesterol into micelles. In mice, abolished synthesis of CA by targeted disruption of the P-450 cytochrome *Cyp8b1* reduces the intestinal cholesterol uptake by about 50% (6). Accordingly, CA-depleted mice also show other effects on cholesterol metabolism: they do not accumulate cholesteryl esters (CEs) in the

Abbreviations: apoE, apolipoprotein E; CA, cholic acid; CE, cholesteryl ester; DKO, double knockout; FC, free cholesterol; FXR, farnesoid X receptor; KO, knockout.

¹K. Slätis and M. Gåfvels contributed equally to this work.

²To whom correspondence should be addressed.

e-mail: mats.gafvels@karolinska.se

^SThe online version of this article (available at <http://www.jlr.org>) contains supplementary data in the form of five figures.

This work was supported by the Swedish Research Council, Medical Branch, the Swedish Heart and Lung Foundation, the County Council of Stockholm, and the Karolinska Institutet Foundations.

Manuscript received 17 June 2010 and in revised form 30 July 2010.

Published, JLR Papers in Press, July 30, 2010

DOI 10.1194/jlr.M009308

Copyright © 2010 by the American Society for Biochemistry and Molecular Biology, Inc.

This article is available online at <http://www.jlr.org>

liver when fed cholesterol-enriched diets (6), and have increased bile acid synthesis and bile acid pool sizes. We have previously shown that in mice, CA also seems to be the most-potent ligand for FXR (7).

To more carefully investigate the role of CA in a condition of disturbed cholesterol metabolism and atherosclerosis, we cross-bred the apoE KO with the *Cyp8b1* knockout (*Cyp8b1* KO) strain (8) to create an experimental mouse model that is prone to developing atherosclerosis but unable to synthesize CA. Our results show that apoE KO mice devoid of CA have only half the amount of atherosclerotic lesions and much lower levels of plasma cholesterol despite upregulated cholesterol synthesis. We also show that the action of CA in this process is most probably confined to formation of intraluminal micelles and, to a minor extent, its potency to activate the nuclear receptor FXR.

MATERIALS AND METHODS

Chemicals

Sodium cholate ($\geq 99\%$) and cholesterol ($>99\%$) were purchased from Sigma-Aldrich, St. Louis, MO. The FXR agonist GW4064 was synthesized by Synthelec, Inc., Forskningsparken Ideon, Lund, Sweden, and was suspended in 1% methylcellulose before administration. [5,6- ^3H] β -sitostanol was obtained from American Radiolabel Chemicals, Inc., St. Louis, MO and [4- ^{14}C] cholesterol from Amersham Biosciences, Sweden.

Animals and experimental procedures

Mice with targeted deletion of *Cyp8b1* (C57/BL6/Sv129 mixed background) were created as reported previously (7). ApoE KO mice on a pure C57/BL6 background were obtained from Taconic, Denmark. Double knockouts (DKOs) for *Cyp8b1* and *apoE* were created by cross-breeding. All DKO animals used in the investigation were obtained by heterozygous breeding, and homozygous apoE KO animals were also generated from the same heterozygous breeding. Groups of four to six males aged 10–20 weeks were age-matched and housed at 22–24°C at a light cycle of 6 AM to 6 PM. Two different diets were given: chow containing 0.025% cholesterol (w/w) (chow diet) or chow supplemented with 0.2% cholesterol (w/w) (cholesterol diet). All diets contained 10% peanut oil (w/w), and water was available ad libitum. Three parallel series of animals were used: apoE KO and DKO mice fed the chow diet for 2 weeks, apoE KO and DKO mice fed the cholesterol diet for 2 weeks, and apoE KO and DKO mice fed the cholesterol diet for 5 months. When using the FXR agonist GW4064, animals were gavaged once daily for 6 days with either the agonist (50 mg/kg/day) or the vehicle (1% methylcellulose). Animals were euthanized by cervical dislocation following CO₂ anesthesia, and the liver and gallbladder were snap-frozen in liquid nitrogen. The small intestine was divided into three equal parts (duodenum, jejunum, and ileum), and the mucosa was scraped and snap-frozen in Trizol (Invitrogen). The heart and the proximal part of the aorta were removed, fixed in 4% formalin in PBS (Sigma-Aldrich) for 1 h and kept frozen until cryosectioning. Blood was collected by heart puncture. All animal studies were approved by the institutional Animal Care and Use Committee at the Karolinska Institute.

Tissue preparation and quantification of atherosclerotic lesions

The heart and ascending aorta were cryosectioned in a standardized manner as previously described (8). Eight 10 μm sec-

tions were collected at 100 μm intervals starting 100 μm distal to the aortic valves. Sections were fixed in formalin and kept at room temperature until stained. Staining was performed with hematoxylin and Oil-Red-O, and lesion size was determined using the Leica QWin image analysis software. Mean cross-section lesion area and total aortic cross-section area were calculated from eight of the sections from each mouse. Sections used for all further analyses were selected within 100 μm from maximal lesion size.

Immunohistochemistry

Sections from the ascending aorta were fixed in ice-cold acetone and stained with any of the following primary antibodies: rat anti-mouse CD68 (Serotec Ltd., UK), biotinylated mouse anti-mouse I-A^b (BD Pharmingen), rat anti-mouse CD3 (Southern Biotechnology Associates), or rat anti-mouse CD106 antibody (BD Pharmingen). For the CD68, CD3, and CD106 staining, primary antibodies were followed by biotinylated anti-rat IgG and were visualized using biotin-avidin-peroxidase complexes (Vector Laboratories). Controls included omission of primary antibodies. CD3+ and I-A+ cells were counted in atherosclerotic lesions, media, and adventitia at $\times 400$ magnification and were expressed as cells/mm². Staining for CD68 and CD106 was registered as stained surface area and expressed as percentage of stained area to total lesion cross-section area. Images of the stained tissues were obtained using laser confocal microscopy with a BioRad MRC 1024 unit attached to a Nikon Diaphot 200 inverted microscope with a Nikon Plan Apo 20 \times and analyzed using Leica Q500MC image analysis software.

Analysis of serum lipoproteins

For analysis of serum lipoproteins, size exclusion chromatography was used (9). Serum total cholesterol, free cholesterol (FC), phospholipids, and triglycerides were determined on-line by standard enzymatic procedures.

Determination of intestinal cholesterol absorption

After feeding the specified diets for 6 days (FXR agonist experiment) or 2 weeks (chow and cholesterol diet), percent cholesterol absorption was assayed by the fecal dual-isotope method, essentially as reported by Schwarz et al. (10), except that feces were collected 24 h after administering the radioactive gavage.

Measurement of hepatic cholesterol, 7 α -hydroxy-4-cholesten-3-one, lathosterol, and bile acids in gallbladder bile

Quantification in liver tissue of FC, total cholesterol, lathosterol, and 7 α -hydroxy-4-cholesten-3-one (C4) was performed as reported (11, 12). Individual bile acid concentrations were determined by gas-liquid chromatography essentially as described (13). Results were expressed as molar percentage of the total bile acid content.

Hepatic acyl-CoA transferase:cholesterol acyltransferase 2 activity

Total acyl-CoA transferase:cholesterol acyltransferase (ACAT) enzymatic activity in liver tissue was determined in microsomal preparations from pooled samples as previously described (14). Piripyropene A, a highly selective ACAT2 inhibitor (14, 15), was used to differentiate between ACAT1 and ACAT2 activity.

mRNA determination by quantitative real-time PCR

Total RNA was isolated with the Quick Prep Total RNA Extraction Kit (Amersham Biosciences, Sweden). Isolation of enterocytic RNA was performed from scraped mucosal cells collected

from the jejunum (the middle third of the small intestine) and ileum (the distal third) and suspended in Trizol (Invitrogen). Oligo-dT-primed cDNA synthesis was carried out on 1 µg of total RNA using the High-Capacity Reverse Transcriptase Kit (Applied Biosystems). Quantitation of pooled cDNA was performed with real-time PCR using fluorochrome-labeled TaqMan probes. Forty-five selected genes were analyzed on a 48-well-format low-density TaqMan array, utilizing the 7900 HT sequence detection system (Applied Biosystems). For measurements of individual *Cyp7a1* and *HMG-CoA reductase* levels, Power SYBR® Green PCR Master Mix (Applied Biosystems) was used with primers overlapping exon-exon boundaries. For detection, Applied Biosystems PRISM 7700 Sequence Detection System instrument and software were used. As an internal standard, mouse hypoxanthine phosphoribosyl transferase was selected.

Statistical analysis

Data are presented as means ± SEM. Statistical analysis was performed with STATISTICA software (StatSoft). The significance of differences was tested by two-way ANOVA, followed by posthoc comparison according to the LSD test. A *P* value <0.05 was considered statistically significant.

RESULTS

Effects of CA depletion on atherosclerosis development

To accelerate the development of atherosclerosis, apoE KO and DKO mice were fed the cholesterol diet for 5 months. Microscopically, typical atherosclerotic lesions occurred in the most proximal part of the ascending aorta, estimated to represent approximately 30% of the aortic area in the apoE KO mice within a zone ranging from 100 to 800 µm distal to the aortic valves. In the DKO animals, the lesion area was approximately 50% smaller compared with the apoE KO mice (Fig. 1). To evaluate any qualitative differences in the atherosclerotic lesions, such as the cellular response, the expressions of various cell surface markers were investigated. No statistically significant difference could be found for the percentage of cells positive for the markers CD3 and I-A^b when comparing the plaques in the DKO mice to those in the apoE KO mice (Table 1). The staining area for the CD68 marker was approximately 30% larger in the DKO mice, whereas no differences were seen for CD106.

Effects of CA depletion on serum lipoproteins

When comparing the apoE KO mice to the DKO mice, the former always had higher levels of FC and CE in the plasma (Table 2). This was especially prominent in the mice fed the cholesterol diet for 5 months, inasmuch as the levels of CE observed in the apoE KO mice were more than 2-fold higher (18.2 vs. 8.2 mmol/l) as compared with the DKO mice. That the dietary treatment also increased the levels of CE in the DKO animals could be seen when comparing their values with those of the DKO mice fed chow diet for 2 weeks (8.2 vs. 3.0 mmol/l). More than 90% of the FC and CE occurred in the apoB-containing lipoprotein fractions, which most probably consisted of chylomicrons and chylomicron remnants (Fig. 2). Alterations in the apoA-I-containing fractions (HDL) were modest.

No significant differences were detected for the triglyceride levels in the lipoprotein profiles when referring to diet regimens and feeding periods.

Effects of CA depletion on the intestinal cholesterol absorption

DKO mice fed the chow diet absorbed approximately 60% less cholesterol compared with the apoE KO animals (see supplementary Fig. 1), which is a pattern similar to that found in *Cyp8b1* KO mice when compared with their corresponding WT animals (7, 11). In animals fed the cholesterol diet for 2 weeks, the total percentage of absorbed cholesterol was reduced in both strains of mice, but still the DKO animals showed approximately 50% less cholesterol absorption (see supplementary Fig. 1).

Effects of CA depletion on the composition of bile and hepatic cholesterol

ApoE KO mice fed the cholesterol diet for either 2 weeks or 5 months showed a prominent increase in their hepatic CE content, in contrast to the DKO mice, which displayed essentially the same levels as found in apoE KO and DKO animals fed a chow diet (Fig. 3A). Thus, the phenotype observed in the *Cyp8b1* KO mice, decreased intestinal cholesterol absorption and lower hepatic CE content, was preserved in the DKO mice. Determination of the hepatic activity of the cholesterol-esterifying enzyme ACAT2 showed that it was much higher in the apoE KO mice than in the DKO mice after 5 months of cholesterol diet feeding, but in animals fed the cholesterol diet for 2 weeks, the difference was not significant (Fig. 3B). No changes were recorded for ACAT1 activity (data not shown). As expected, the percentage of CA in primary bile was negligible in the DKO mice, which consistently was compensated for by an increase of β-muricholic acid and chenodeoxycholic/α-muricholic acid (Table 3).

Effects of CA depletion on bile acid and cholesterol metabolism

The hepatic C4/total cholesterol ratio, an indicator of bile acid synthesis, was significantly higher in the DKO compared with the apoE KO mice in all diet groups (Fig. 4A). A similar pattern was found for *Cyp7a1* mRNA expression (Fig. 4B), indicating that the bile acid synthesis was much more intensive in the DKO animals. Furthermore, the cholesterol diet did not change this pattern. No differences were recorded for the mRNA levels of *Cyp27* and *Cyp7b1* in DKO or apoE KO mice when comparing the chow diet to the cholesterol diet in the 2 week feeding period (see supplementary Fig. II). Determination of the hepatic lathosterol/total cholesterol ratio, reflecting de novo cholesterol synthesis in the liver, showed that there were no significant differences between DKO and apoE KO mice when fed a chow diet (Fig. 4C). In apoE KO mice fed the cholesterol diet, the ratio of lathosterol/total cholesterol was reduced compared with the apoE KO mice fed the chow diet. In contrast, the DKO mice showed no significant differences after 2 weeks of cholesterol diet feeding, whereas a modest reduction was obtained after 5 months. The mRNA levels for *HMG-CoA reductase* demonstrated a

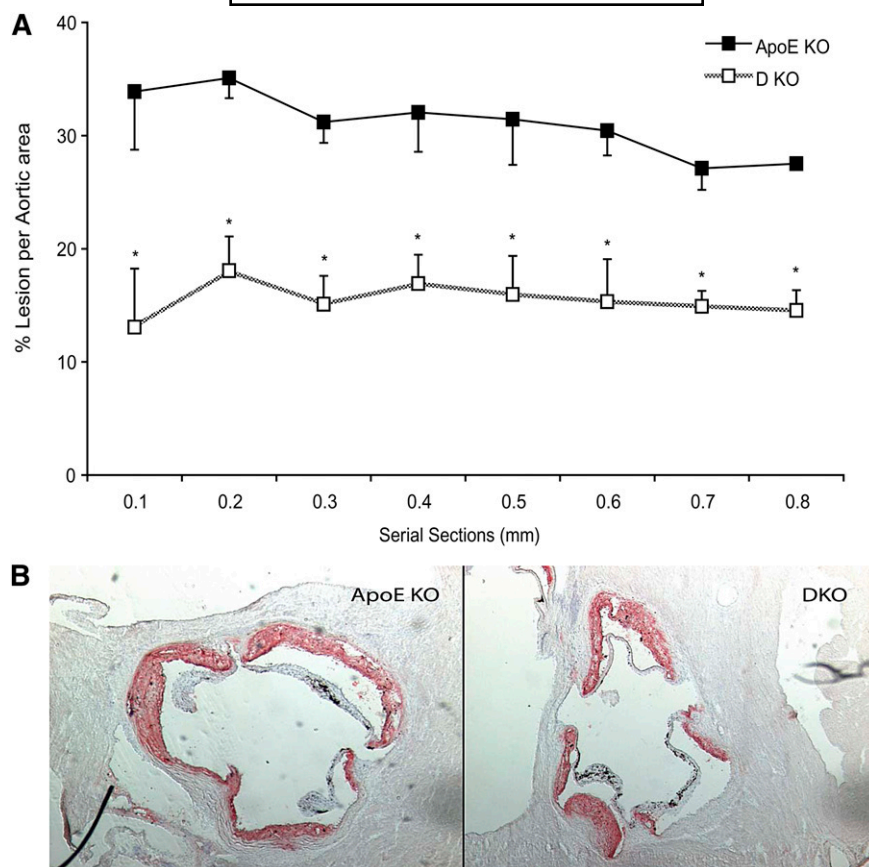


Fig. 1. A: Percentage of atherosclerotic lesion area as measured by Oil-Red-O staining on different levels in the aorta in apolipoprotein E knockout (apoE KO) and double knockout (DKO) mice. The mice were fed a cholesterol diet for 5 months. Serial sections of 0.1 mm were analyzed starting 0.1 mm distal to the aortic valve. * Statistically significant difference from the corresponding serial section in apoE KO mice, $P < 0.05$. B: Atherosclerotic lesions in the same section of the proximal aorta from an apoE KO mouse (left) and a DKO mouse (right). Lesions were stained with Oil-Red-O and hematoxylin. Data are presented as mean \pm SEM.

similar pattern, with suppression in apoE KO mice fed the cholesterol diet and modest alterations in the DKO mice (Fig. 4B). No significant alterations were found for the mRNA levels corresponding to other hepatic genes involved in the bile acid and cholesterol metabolism in the DKO and apoE KO mice when comparing the chow diet to the cholesterol diet (2 week feeding period) or when comparing the DKO to the apoE KO mice in both diet groups: *ApoA1*, *Abca1*, *ApoC2*, *Ldl-receptor*, *Ntcp*, *Abcb4*, *Acat2*, *Fxr*, and *Lxra* (see supplementary Figs. II, III). A reduction was observed in hepatic *Abcg5/g8* mRNA expression in DKO

compared with apoE KO mice after 2 weeks of cholesterol diet, possibly due to less accumulation of cholesterol in the liver. A similar pattern was observed after 5 months of cholesterol diet (data not shown).

Of the genes occurring in the distal ileum, *Fgf15* mRNA levels were reduced more than 50% in the DKO mice compared with the apoE KO mice after both 2 weeks and 5 months of the cholesterol diet. This would be a consequence of abolished CA synthesis in the DKO mice, inasmuch as *Fgf15* gene expression is upregulated via FXR, and furthermore, it would explain why *Cyp7a1* mRNA levels were higher in the DKO mice. No differences were observed in the mRNA expressions for *Abcg5/g8*, *Abca1*, *Lxra* and β , or *Fxr* in jejunum or for *Ibapb* or *Asbt* in ileum with respect to genotype after 2 weeks of cholesterol diet feeding (see supplementary Fig. IV), and a similar pattern was observed after 5 months (data not shown).

Effects of FXR agonist treatment on CA-depleted mice

To differentiate between the micellar and FXR signaling effects of CA, groups of DKO mice were treated either with dietary CA (0.2% w/w) or with the synthetic FXR agonist GW4064 (50 mg/kg/day). Administration of GW4064 did not change the intestinal cholesterol uptake, whereas

TABLE 1. Expression of cell surface markers in proximal aorta

	ApoE KO	DKO
Cells/lesion area (cells/mm ²)		
CD3	88 \pm 9	214 \pm 79
IA ^b	252 \pm 57	352 \pm 115
Stained area/lesion area (%)		
CD68	26 \pm 3	34 \pm 6*
CD106	53 \pm 4	59 \pm 4

ApoE KO, apolipoprotein E knockout; DKO, double knockout. * Statistically significant difference from apoE KO, $P < 0.05$. All values are mean \pm SEM (n = 4). Mice were treated with a cholesterol diet for 5 months.

TABLE 2. Levels of cholesterol, triglycerides, and phospholipids in serum

Serum Lipids (mmol/l)		Total Particles		ApoB Particles		ApoA-I Particles	
		ApoE KO	DKO	ApoE KO	DKO	Apo E KO	DKO
Chow diet 2 weeks	TC	12.7 ± 1.9	5.5 ± 0.9	11.2 ± 1.9	4.6 ± 0.7	1.5 ± 0.1	0.9 ± 0.2*
	FC	5.6 ± 0.6	3.5 ± 1.1	4.8 ± 0.5	3.1 ± 0.2	0.8 ± 0.2	0.4 ± 0.1
	CE	7.3 ± 0.4	3.0 ± 0.3	6.5 ± 0.5	2.4 ± 0.3	0.7 ± 0.2	0.6 ± 0.0
	TG	1.9 ± 0.6	1.2 ± 0.2	1.6 ± 0.5	1.1 ± 0.3	0.3 ± 0.2	0.1 ± 0.5
	PL	20.8 ± 1.3	18.4 ± 3.6	12.4 ± 0.7	10.9 ± 2.3	8.4 ± 0.7	7.5 ± 1.3
Cholesterol diet 2 weeks	TC	22.4 ± 3.0	14.7 ± 2.7*	21.7 ± 3.1	13.5 ± 2.7*	0.6 ± 0.3	1.3 ± 0.2*
	FC	7.1 ± 0.5	5.5 ± 0.4	6.9 ± 0.5	5.1 ± 0.4	0.2 ± 0.1	0.4 ± 0.0
	CE	15.3 ± 0.9	9.2 ± 1.0*	14.8 ± 1.0	8.4 ± 1.0*	0.5 ± 0.1	0.9 ± 0.1
	TG	0.6 ± 0.1	1.1 ± 0.0	0.5 ± 0.1	0.9 ± 0.0	0.1 ± 0.0	0.1 ± 0.0
	PL	21.4 ± 2.0	17.0 ± 1.0	17.0 ± 1.6	11.5 ± 0.7	4.4 ± 0.7	5.6 ± 0.4
Cholesterol diet 5 months	TC	26.8 ± 4.4	13.5 ± 3.2*	25.9 ± 4.3	12.4 ± 3.2*	0.9 ± 0.2	1.2 ± 0.1
	FC	8.7 ± 0.6	5.3 ± 0.5*	8.3 ± 0.5	4.9 ± 0.4*	0.3 ± 0.1	0.4 ± 0.1
	CE	18.2 ± 1.7	8.2 ± 1.5*	17.5 ± 1.9	7.4 ± 1.4*	0.6 ± 0.1	0.8 ± 0.0
	TG	1.0 ± 0.2	1.1 ± 0.3	1.0 ± 0.2	1.0 ± 0.3	0.1 ± 0.0	0.1 ± 0.1
	PL	22.1 ± 1.4	16.8 ± 1.1	18.0 ± 1.1	12.1 ± 0.6	4.0 ± 0.3	4.8 ± 1.1

Serum concentration of lipids. TC, total cholesterol; FC, free cholesterol; CE, cholesteryl ester; TG, triglyceride; PL, phospholipid in mmol/l of apoE KO and DKO animals fed a chow diet for 2 weeks or a cholesterol diet for 2 weeks or 5 months. The results are expressed as mean ± SEM (n = 4–5). * Statistically significant difference from apoE KO with the same diet, $P < 0.05$.

addition of CA markedly increased the intestinal cholesterol absorption to the same level seen in apoE KO animals (Fig. 5A). Treatments with both GW4064 and CA upregulated the *Fgf15* mRNA in the ileum, but the strongest response was obtained with the synthetic agonist (Fig. 5B). In addition, a prominent induction of *Shp* mRNA was found for GW4064, but much less for CA. Expression of *Npc1l1* in jejunum and ileum was essentially unchanged by the CA and GW4064 treatment in the DKO mice, and mRNA levels for *Abcg5/g8* were also unaffected by the GW4064 treatment. Thus, the cholesterol absorption in this experiment did not correlate with the *Npc1l1* expression, but rather with the presence or absence of CA, which might reflect that the main effect of CA for cholesterol absorption is due to its micellar-forming properties.

GW4064 did not induce any changes in the total plasma cholesterol concentrations compared with the vehicle-gavaged animals, but, in contrast, CA restored the total cholesterol levels in all plasma fractions to a pattern similar to that occurring in untreated apoE KO mice (data not shown). Nor did the FXR agonist treatment affect the levels of hepatic CE when compared with vehicle-treated animals (data not shown). Treatment with both CA and GW4064 decreased the mRNA levels for *HMG-CoA reductase*, *HMG-CoA synthase*, and *Cyp7a1*, indicating a down-regulation of cholesterol and bile acid synthesis (Fig. 5C). GW4064 administration also reduced the amount of chenodeoxycholic/ α -muricholic acid in the bile, whereas the amount of β -muricholate increased (Table 3).

DISCUSSION

Not only do bile acids facilitate the uptake of dietary lipids, they also exert endocrine and paracrine effects within various areas of the metabolism. In addition to the micellar-forming ability in the intestine, CA also functions as a specific ligand for FXR (2). Mice with an inhibited synthesis of CA have several phenotypic features: decreased cholesterol

absorption, increased synthesis of bile acids and cholesterol, and resistance to hepatic accumulation of CEs. The present study is the first to demonstrate the effects of abolished CA synthesis on lipid metabolism and atherosclerotic progression in the apoE-deficient mouse, a well-known animal model for the studies of cardiovascular diseases.

Compared with apoE KO animals, the extent of atherosclerotic lesions in DKO animals was 50% less. Analysis of the cellular markers CD106 (VCAM-1), CD3, and I-A^b in the lesions indicated that no essential differences occurred between the two groups in the local inflammatory process. The DKO mice displayed lower levels of cholesterol in their apoB-containing lipoproteins, upregulated bile acid synthesis, and less accumulation of CE in the liver. Because no significant changes occurred in the cholesterol levels of the apoA-I-containing lipoprotein particles, we can assume that the major part of the absorbed cholesterol ends up in apoB-containing lipoproteins. This particular fraction consists mainly of chylomicron remnants, inasmuch as the deficiency of apoE seriously hampers their receptor-mediated uptake into the liver, and furthermore, it is reported that the hepatic release of VLDL particles in those mice is decreased (16). Compared with the apoE KO animals, the DKO mice displayed approximately 50% lower levels of plasma CE in their apoB-containing fractions, which seems to be due to the diminished uptake of intestinal cholesterol in these mice. Actually, DKO mice fed the cholesterol diet displayed levels of CE in their apoB-containing lipoproteins similar to those seen in apoE KO mice on the chow diet (containing 0.025% cholesterol or 1/8 of the cholesterol amount in the cholesterol diet). As a consequence, we could estimate that depletion of CA confers resistance to a diet containing at least eight times more cholesterol.

The relationship between intestinal cholesterol absorption and atherosclerotic development in apoE KO mice has been investigated using several approaches: treatment with ezetimibe (17) or genetic depletion of NPC1L1 (18) or ACAT2 (19). In all cases, a prominent reduction of

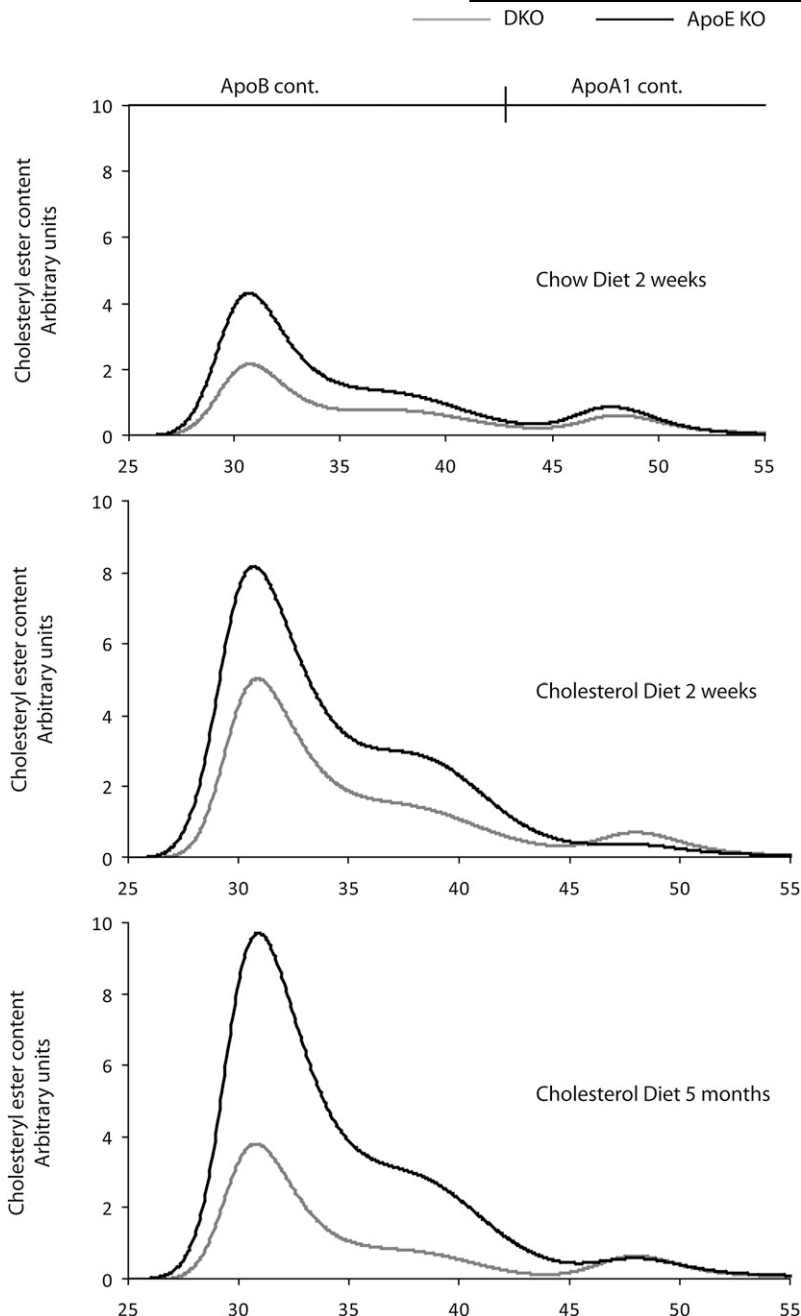


Fig. 2. Lipoprotein profiles in serum by size-exclusion chromatography. Relative cholesteryl ester content in serum of apoE KO and DKO animals fed a chow diet for 2 weeks or cholesterol diet for 2 weeks or 5 months.

Downloaded from www.jlr.org by guest, on June 14, 2012

cholesterol absorption was demonstrated, accompanied by a significant decrease of atherosclerotic lesions. Ezetimibe treatment and genetic depletion of NPC1L1 probably affect the same uptake mechanism within the enterocyte, and the mode of action is limited to the direct absorptive process. Targeted disruption of *Npc1l1* in apoE KO mice reduces the total cholesterol absorption by 60–70% (20, 21) and the atherosclerotic lesions by >90% (22). Elimination of CA decreases the uptake to barely half, corresponding to a total cholesterol absorption of around 30%, and reduces atherosclerotic lesions by 50%. However, the atheroprotective effect seems to vary in different apoE mouse models, inasmuch as even a modest reduction of 41% of the intestinal cholesterol absorption achieved a 70% decrease of the atherosclerosis formation (23). It is

nevertheless remarkable that the intestinal cholesterol absorption in our DKO mice was not reduced even more; Wang et al. (24) demonstrated that mice with high levels of muricholic acids in their bile (80–85%) only absorbed 11–12% of luminal cholesterol. One possible explanation could be that the bile acid pool of the *Cyp8b1*-deficient animals is expanded and contains slightly more hydrophobic bile acid and less (~75%) muricholic acid. An increased uptake of bile acid in the distal ileum is less probable, inasmuch as no alterations were observed in the mRNA for bile acid transporters.

Earlier studies have suggested that FXR agonist treatment could be responsible for suppression of intestinal cholesterol absorption in the mouse (25). However, treatment of DKO mice with the synthetic FXR agonist GW4064

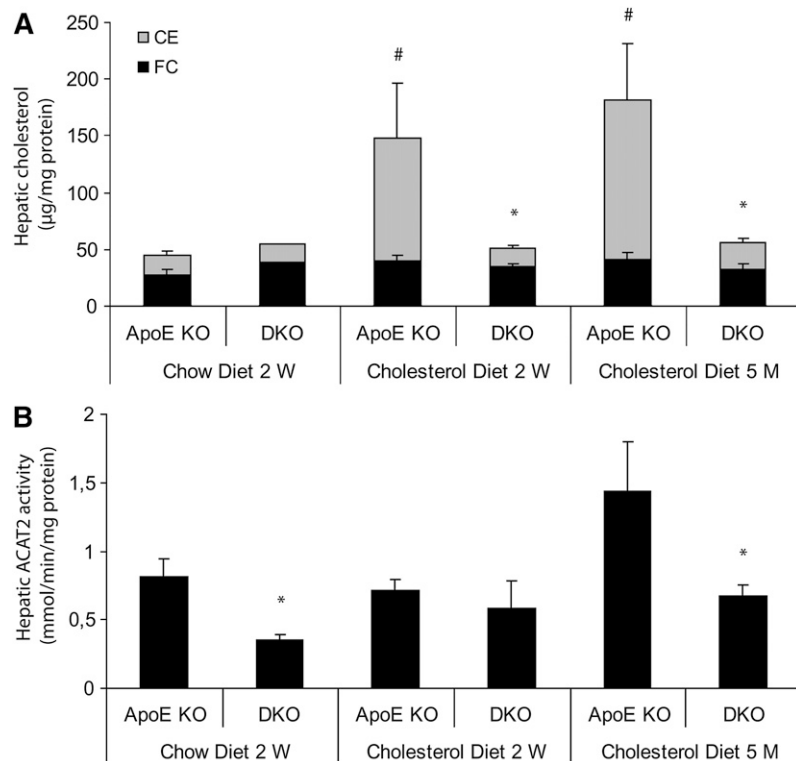


Fig. 3. A: Levels of total hepatic cholesterol, free cholesterol (FC), and cholesteryl esters (CEs) of apoE KO versus DKO animals fed a chow diet for 2 weeks (2 W) or a cholesterol diet for 2 weeks or 5 months (5 M). # Statistically significant difference from apoE KO mice fed a chow diet for 2 weeks. * Statistically significant difference from apoE KO mice fed a cholesterol diet for 5 months, $P < 0.05$. B: Effects of cholic acid (CA) depletion on the hepatic ACAT2 activity in apoE KO versus DKO animals fed a chow diet for 2 weeks or a cholesterol diet for 2 weeks or 5 months. * Statistically significant difference from apoE KO mice on the corresponding diet, $P < 0.05$. Data are presented as mean \pm SEM.

did not restore the intestinal absorptive capacity (or induce any changes in the intestinal cholesterol absorption), whereas in fact, addition of 0.2% CA did. Our results showed that both GW4064 and CA increased the transcription of several target genes for FXR, such as *Shp* and *Fgf15*, whereby the peptide coded for by the latter would downregulate the *Cyp7a1* transcription (11). The major function for CA in the cholesterol absorptive process would thus be restricted to the formation of appropriate micelles, rather than ability to modulate the expression of FXR-regulated genes. This view is supported by the finding that the intestinal expression of *Npc1l1* was unaffected by the administration of CA or GW4064. Furthermore, *Abcg5/g8* expression was not affected by GW4064 in the DKO mice, suggesting that the FXR agonist did not affect the net uptake of cholesterol into the enterocytes.

Our results show that four characteristic features of the *Cyp8b1* KO phenotype were preserved in the DKO animals: upregulated bile acid and de novo cholesterol synthesis in the liver, reduced intestinal cholesterol absorption, and reduced accumulation of hepatic CE. Even if the DKO mice synthesize larger quantities of bile acids from cholesterol, most of the production consists of muricholic acid, being much less efficient in carrying out micellar formation, and thus cholesterol absorption (24, 26), and FXR-mediated signaling. This might explain why DKO mice have lower hepatic CE levels and decreased ACAT2 activity, compared with apoE KO mice, even when the former are kept on a cholesterol diet and have a higher rate of cholesterol synthesis. Elimination of the FXR agonist CA seems to decrease the production of FGF15, which might be the main reason why *Cyp7a1* is upregulated, a finding

TABLE 3. Bile acid composition of gallbladder bile

Bile Acid Composition (% of Total Bile Acids)		DCA	CDCA + α -Muricholic Acid	CA	UDCA	β -Muricholic Acid
Chow diet 2 weeks	ApoE KO	<1	5.3 \pm 1.7	52.0 \pm 3.8	<1	42.5 \pm 4.0
	DKO	<1	24.8 \pm 1.9*	<1*	3.5 \pm 2.0*	71.7 \pm 3.5*
Cholesterol diet 5 months	ApoE KO	1.6 \pm 0.6	8.8 \pm 0.4	51.2 \pm 1.4	1.0 \pm 0.6	37.4 \pm 1.8
	DKO	<1	36.9 \pm 2.9*	<1*	8.1 \pm 0.7*	47.8 \pm 2.5
Chow diet 6 days	ApoE KO	1.0 \pm 0.6	2.2 \pm 1.0	64.3 \pm 1.1	<1	32.8 \pm 1.5
	DKO	<1	25.6 \pm 0.8 [†]	2.8 \pm 2.8 [†]	9.1 \pm 0.8 [†]	62.6 \pm 2.1 [†]
Chow diet 6 days + GW4064	DKO	<1	10.5 \pm 6.2	<1 [†]	4.8 \pm 2.8 [†]	84.4 \pm 9.1 [†]
	DKO	3.6 \pm 1.8	3.4 \pm 1.4	72.9 \pm 9.4	1.7 \pm 1.3	18.4 \pm 8.5

The results are expressed as mean \pm SEM (n = 3–5). Values represent percent (%) of total gallbladder bile acids. Before euthanization, the mice were fasted for 4 h. CDCA, chenodeoxycholic acid; UDCA, ursodeoxycholic acid; DCA, deoxycholic acid. * Statistically significant difference from apoE KO with the same diet. [†] Statistically significant difference from apoE KO chow diet for 6 days, $P < 0.05$.

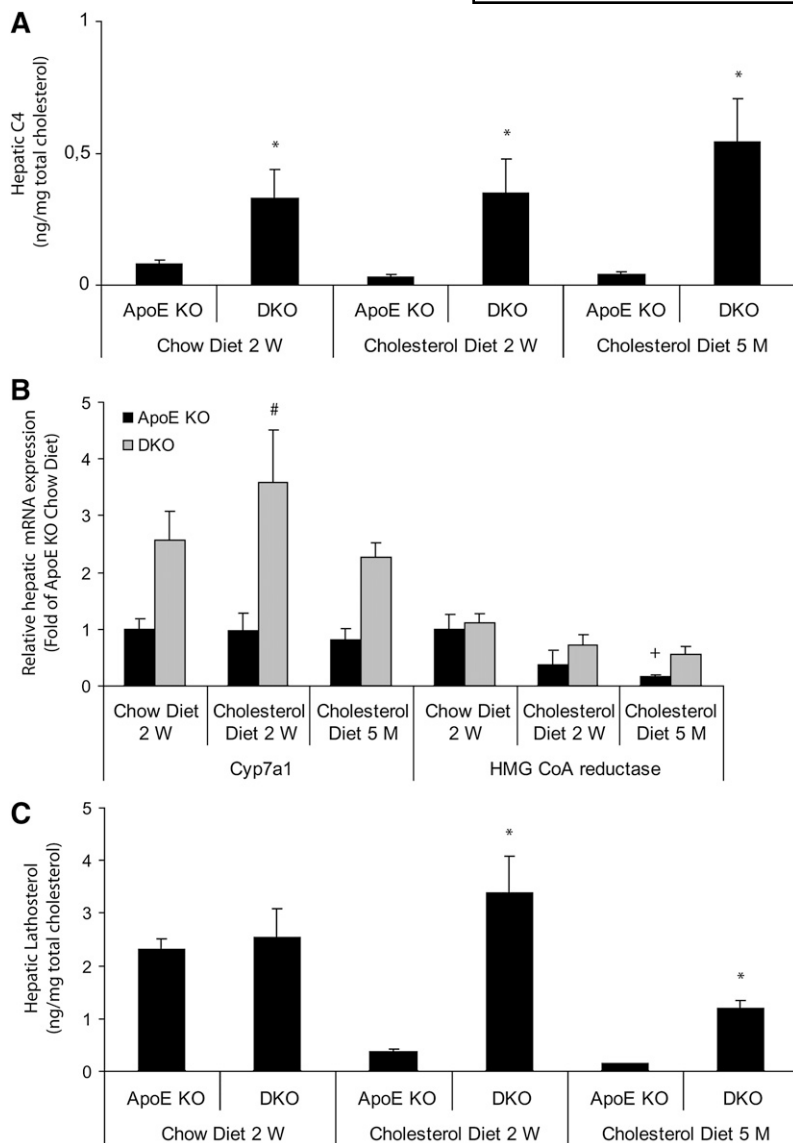


Fig. 4. Effects of CA depletion on hepatic bile acid and cholesterol synthesis. A: 7 α -Hydroxy-4-cholesten-3-one (C4) content, related to hepatic total cholesterol levels. * Statistically significant difference from apoE KO mice treated with the corresponding diet, $P < 0.05$. B: mRNA levels of the hepatic genes *Cyp7a1* and *HMG-CoA reductase*, related to the corresponding mRNA levels of apoE KO mice fed a chow diet for 2 weeks (2 W). # Statistically significant difference from apoE KO mice fed a chow diet for 2 weeks, $P < 0.05$. + Statistically significant difference from DKO mice fed a chow diet for 2 weeks, $P < 0.05$. C: Hepatic lathosterol concentrations, as related to hepatic total cholesterol content. * Statistically significant difference from apoE KO mice treated with the corresponding diet, $P < 0.05$. Data are presented as mean \pm SEM.

which is in accordance with the obtained hepatic C4/total cholesterol values. Our results also demonstrated that the bile acid synthesis of the apoE KO mice was not enhanced by the cholesterol diet, which might explain their hepatic accumulation of CE.

Addition of cholesterol to the diet is reported to increase *Cyp7a1* mRNA expression and consequently, bile acid synthesis (27). However, our animals fed the 0.2% cholesterol diet did not upregulate their *Cyp7a1* expression. One reason may be that previous studies utilized diets containing 2% cholesterol, whereas diets with 0.2% cholesterol have not been extensively applied. With treatment of WT and apoE KO mice with a 2% cholesterol diet, the mean values of the *Cyp7a1* mRNA levels doubled, although statistical significance was not reached, owing to large interindividual variations, whereas the 0.2% cholesterol diet did not induce any apparent changes (see supplementary Fig. V). The *Cyp7a1* mRNA levels of the DKO mice were not affected by the diets, probably because *Cyp7a1* already was highly upregulated in these mice. Even if the 0.2% cholesterol diet did not increase the mRNA

levels of *Cyp7a1*, the dose was nevertheless able to induce plaque formation in the apoE KO and DKO animals.

The effect of ezetimibe in humans is not as prominent as in mice; treatment of mildly hypercholesterolemic patients reduced the cholesterol absorption an average of 54% (28). Nevertheless, today, inhibition of cholesterol absorption by ezetimibe is one of the major therapeutic alternatives for treatment of cardiovascular diseases, although until now, long-term studies in large patient groups have not been available. In recent clinical studies, the impact on cardiovascular events with ezetimibe treatment was less than expected (29). In humans, large interindividual variations exist between the proportions of CA and chenodeoxycholic acid, the other major bile acid (30), and studies evaluating the effect of CA on intestinal cholesterol absorption show contradictory results. In some investigations, administration of CA did not change the absorption (31, 32), whereas in others, an increase was reported (33). Reduced CA production by administration of an appropriate inhibitor to the CYP8B1 P-450 cytochrome may offer yet another possibility to diminish cholesterol

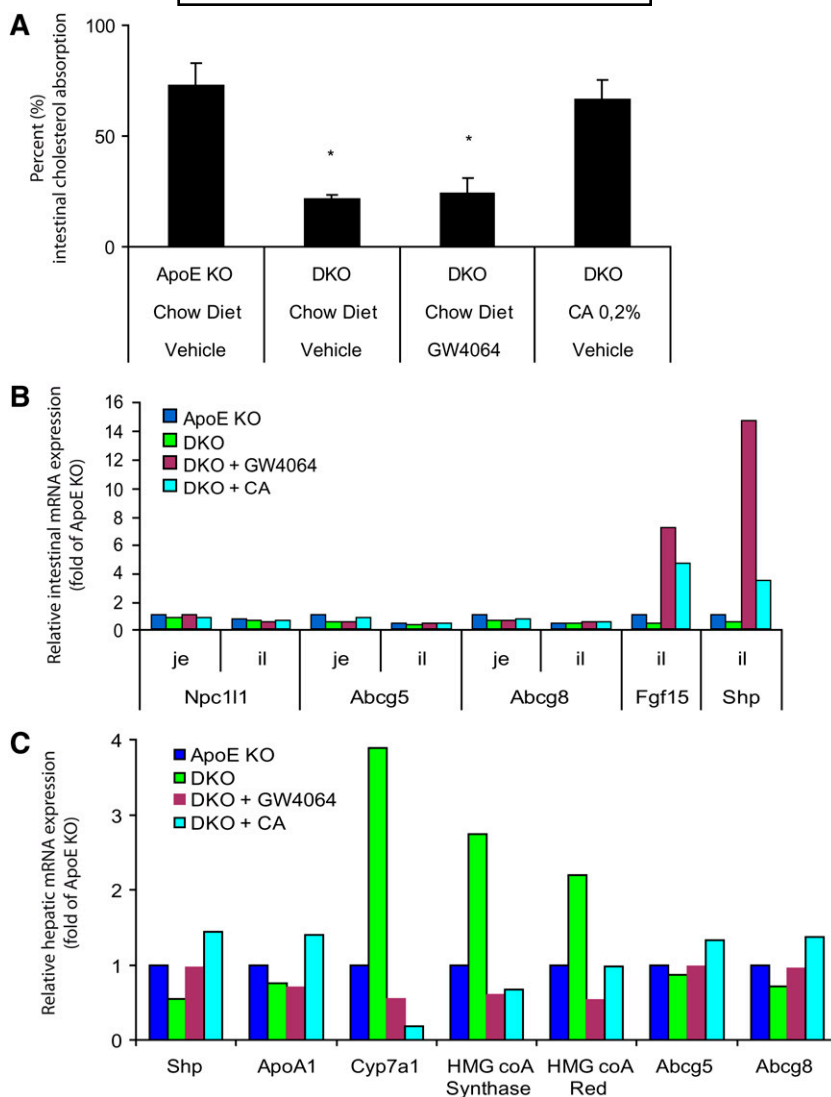



Fig. 5. Effects of treatment of DKO and apoE KO animals with the farnesoid X receptor agonist GW4064 or 0.2% CA. The animals were treated for 6 days with GW4064 (50 mg/kg/day), vehicle (1% methylcellulose), or CA (0.2%). **A:** Intestinal cholesterol absorption. * Statistically significant difference from apoE KO, $P < 0.05$. **B:** Relative mRNA levels of intestinal genes involved in cholesterol transport and signaling in pooled samples from jejunum (je) and ileum (il) of the small intestine. **C:** Relative mRNA levels of genes involved in cholesterol and bile acid synthesis and transport in pooled hepatic samples. Data are presented as mean \pm SEM.

absorption. Presently, it is not possible to foresee all the effects in humans following a decreased synthesis of CA, although reduced cholesterol absorption would be expected. Because chenodeoxycholic acid seems to be the primary FXR ligand in humans (34), it is difficult to speculate about the metabolic consequences of such an approach, or about whether higher proportions of chenodeoxycholic acid in the bile might alter the release of FGF19 with consequences for bile acid production. Inhibition of CYP8B1 might also be considered for treatment of other diseases with disturbed cholesterol homeostasis like gallstone disease, because gallstone formation might be prevented by depleting CA (11). 

The authors are deeply indebted to Dr. Johan Malm, Actar AB, who provided us with the FXR agonist GW4064.

REFERENCES

- Ross, R. 1999. Atherosclerosis—an inflammatory disease. *N. Engl. J. Med.* **340**: 115–126.
- Lefebvre, P., B. Cariou, F. Lien, F. Kuipers, and B. Staels. 2009. Role of bile acids and bile acid receptors in metabolic regulation. *Physiol. Rev.* **89**: 147–191.
- Plump, A. S., J. D. Smith, T. Hayek, K. Aalto-Setälä, A. Walsh, J. G. Verstuyft, E. M. Rubin, and J. L. Breslow. 1992. Severe hypercholesterolemia and atherosclerosis in apolipoprotein E-deficient mice created by homologous recombination in ES cells. *Cell.* **71**: 343–353.
- Meir, K. S., and E. Leitersdorf. 2004. Atherosclerosis in the apolipoprotein-E-deficient mouse: a decade of progress. *Arterioscler. Thromb. Vasc. Biol.* **24**: 1006–1014.
- Davis, H. R., Jr., and S. W. Altmann. 2009. Niemann-Pick C1 Like 1 (NPC1L1) an intestinal sterol transporter. *Biochim. Biophys. Acta.* **1791**: 679–683.
- Murphy, C., P. Parini, J. Wang, I. Bjorkhem, G. Eggertsen, and M. Gafvels. 2005. Cholic acid as key regulator of cholesterol synthesis, intestinal absorption and hepatic storage in mice. *Biochim. Biophys. Acta.* **1735**: 167–175.

7. Li-Hawkins, J., M. Gafvels, M. Olin, E. G. Lund, U. Andersson, G. Schuster, I. Bjorkhem, D. W. Russell, and G. Eggertsen. 2002. Cholic acid mediates negative feedback regulation of bile acid synthesis in mice. *J. Clin. Invest.* **110**: 1191–1200.
8. Robertson, A. K., M. Rudling, X. Zhou, L. Gorelik, R. A. Flavell, and G. K. Hansson. 2003. Disruption of TGF-beta signaling in T cells accelerates atherosclerosis. *J. Clin. Invest.* **112**: 1342–1350.
9. Parini, P., L. Johansson, A. Broijerssen, B. Angelin, and M. Rudling. 2006. Lipoprotein profiles in plasma and interstitial fluid analyzed with an automated gel-filtration system. *Eur. J. Clin. Invest.* **36**: 98–104.
10. Schwarz, M., D. W. Russell, J. M. Dietschy, and S. D. Turley. 1998. Marked reduction in bile acid synthesis in cholesterol 7alpha-hydroxylase-deficient mice does not lead to diminished tissue cholesterol turnover or to hypercholesterolemia. *J. Lipid Res.* **39**: 1833–1843.
11. Wang, J., C. Einarsson, C. Murphy, P. Parini, I. Bjorkhem, M. Gafvels, and G. Eggertsen. 2006. Studies on LXR- and FXR-mediated effects on cholesterol homeostasis in normal and cholic acid-depleted mice. *J. Lipid Res.* **47**: 421–430.
12. Lovgren-Sandblom, A., M. Heverin, H. Larsson, E. Lundstrom, J. Wahren, U. Diczfalusy, and I. Bjorkhem. 2007. Novel LC-MS/MS method for assay of 7alpha-hydroxy-4-cholesten-3-one in human plasma. Evidence for a significant extrahepatic metabolism. *J. Chromatogr. B Analyt. Technol. Biomed. Life Sci.* **856**: 15–19.
13. Angelin, B., and B. Leijd. 1980. Effects of cholic acid on the metabolism of endogenous plasma triglyceride and on biliary lipid composition in hyperlipoproteinemia. *J. Lipid Res.* **21**: 1–9.
14. Parini, P., M. Davis, A. T. Lada, S. K. Erickson, T. L. Wright, U. Gustafsson, S. Sahlin, C. Einarsson, M. Eriksson, B. Angelin, et al. 2004. ACAT2 is localized to hepatocytes and is the major cholesterol-esterifying enzyme in human liver. *Circulation.* **110**: 2017–2023.
15. Lada, A. T., M. Davis, C. Kent, J. Chapman, H. Tomoda, S. Omura, and L. L. Rudel. 2004. Identification of ACAT1- and ACAT2-specific inhibitors using a novel, cell-based fluorescence assay: individual ACAT uniqueness. *J. Lipid Res.* **45**: 378–386.
16. Maugeais, C., U. J. Tietge, K. Tsukamoto, J. M. Glick, and D. J. Rader. 2000. Hepatic apolipoprotein E expression promotes very low density lipoprotein-apolipoprotein B production in vivo in mice. *J. Lipid Res.* **41**: 1673–1679.
17. Davis, H. R., Jr., D. S. Compton, L. Hoos, and G. Tetzloff. 2001. Ezetimibe, a potent cholesterol absorption inhibitor, inhibits the development of atherosclerosis in ApoE knockout mice. *Arterioscler. Thromb. Vasc. Biol.* **21**: 2032–2038.
18. Davis, H. R., Jr., L. M. Hoos, G. Tetzloff, M. Maguire, L. J. Zhu, M. P. Graziano, and S. W. Altmann. 2007. Deficiency of Niemann-Pick C1 Like 1 prevents atherosclerosis in ApoE^{-/-} mice. *Arterioscler. Thromb. Vasc. Biol.* **27**: 841–849.
19. Willner, E. L., B. Tow, K. K. Buhman, M. Wilson, D. A. Sanan, L. L. Rudel, and R. V. Farese, Jr. 2003. Deficiency of acyl CoA:cholesterol acyltransferase 2 prevents atherosclerosis in apolipoprotein E-deficient mice. *Proc. Natl. Acad. Sci. USA.* **100**: 1262–1267.
20. Davis, H. R., Jr., L. J. Zhu, L. M. Hoos, G. Tetzloff, M. Maguire, J. Liu, X. Yao, S. P. Iyer, M. H. Lam, E. G. Lund, et al. 2004. Niemann-Pick C1 Like 1 (NPC1L1) is the intestinal phytosterol and cholesterol transporter and a key modulator of whole-body cholesterol homeostasis. *J. Biol. Chem.* **279**: 33586–33592.
21. Altmann, S. W., H. R. Davis, Jr., L. J. Zhu, X. Yao, L. M. Hoos, G. Tetzloff, S. P. Iyer, M. Maguire, A. Golovko, M. Zeng, et al. 2004. Niemann-Pick C1 Like 1 protein is critical for intestinal cholesterol absorption. *Science.* **303**: 1201–1204.
22. Yu, L., S. Bharadwaj, J. M. Brown, Y. Ma, W. Du, M. A. Davis, P. Michaely, P. Liu, M. C. Willingham, and L. L. Rudel. 2006. Cholesterol-regulated translocation of NPC1L1 to the cell surface facilitates free cholesterol uptake. *J. Biol. Chem.* **281**: 6616–6624.
23. Facenbergh, M. E., J. D. Smith, and E. Shayek. 2009. Moderately decreased cholesterol absorption rates are associated with a large atheroprotective effect. *Arterioscler. Thromb. Vasc. Biol.* **29**: 1745–1750.
24. Wang, D. Q., S. Tazuma, D. E. Cohen, and M. C. Carey. 2003. Feeding natural hydrophilic bile acids inhibits intestinal cholesterol absorption: studies in the gallstone-susceptible mouse. *Am. J. Physiol. Gastrointest. Liver Physiol.* **285**: G494–G502.
25. Lambert, G., M. J. Amar, G. Guo, H. B. Brewer, Jr., F. J. Gonzalez, and C. J. Sinal. 2003. The farnesoid X-receptor is an essential regulator of cholesterol homeostasis. *J. Biol. Chem.* **278**: 2563–2570.
26. Zhang, Y., X. Wang, C. Vales, F. Y. Lee, H. Lee, A. J. Lusis, and P. A. Edwards. 2006. FXR deficiency causes reduced atherosclerosis in Ldlr^{-/-} mice. *Arterioscler. Thromb. Vasc. Biol.* **26**: 2316–2321.
27. Peet, D. J., S. D. Turley, W. Ma, B. A. Janowski, J. M. Lobaccaro, R. E. Hammer, and D. J. Mangelsdorf. 1998. Cholesterol and bile acid metabolism are impaired in mice lacking the nuclear oxysterol receptor LXR alpha. *Cell.* **93**: 693–704.
28. Sudhop, T., D. Lutjohann, A. Kodal, M. Igel, D. L. Tribble, S. Shah, I. Perevovskaya, and K. von Bergmann. 2002. Inhibition of intestinal cholesterol absorption by ezetimibe in humans. *Circulation.* **106**: 1943–1948.
29. Kastelein, J. J., F. Akdim, E. S. Stroes, A. H. Zwinderman, M. L. Bots, A. F. Stalenhoef, F. L. Visseren, E. J. Sijbrands, M. D. Trip, E. A. Stein, et al. 2008. Simvastatin with or without ezetimibe in familial hypercholesterolemia. *N. Engl. J. Med.* **358**: 1431–1443.
30. Reihner, E., I. Bjorkhem, B. Angelin, S. Ewerth, and K. Einarsson. 1989. Bile acid synthesis in humans: regulation of hepatic microsomal cholesterol 7 alpha-hydroxylase activity. *Gastroenterology.* **97**: 1498–1505.
31. Einarsson, K., and S. M. Grundy. 1980. Effects of feeding cholic acid and chenodeoxycholic acid on cholesterol absorption and hepatic secretion of biliary lipids in man. *J. Lipid Res.* **21**: 23–34.
32. Sama, C., and N. F. LaRusso. 1982. Effect of deoxycholic, chenodeoxycholic, and cholic acids on intestinal absorption of cholesterol in humans. *Mayo Clin. Proc.* **57**: 44–50.
33. Woollett, L. A., D. D. Buckley, L. Yao, P. J. Jones, N. A. Granholm, E. A. Tolley, P. Tso, and J. E. Heubi. 2004. Cholic acid supplementation enhances cholesterol absorption in humans. *Gastroenterology.* **126**: 724–731.
34. Ellis, E., M. Axelson, A. Abrahamsson, G. Eggertsen, A. Thorne, G. Nowak, B. G. Ericzon, I. Bjorkhem, and C. Einarsson. 2003. Feedback regulation of bile acid synthesis in primary human hepatocytes: evidence that CDCA is the strongest inhibitor. *Hepatology.* **38**: 930–938.